CORA Cork Open Research Archive
Cartlann Taighde Oscailte Chorcaí

Title	Integrated demultiplexing and amplification of coherent optical combs
Authors	Cotter, William E.;Morrissey, Padraic. E.;Yang, Hua;O'Callaghan, James;Roycroft, Brendan;Corbett, Brian M.;Peters, Frank H.
Publication date	2019-05-27
Original Citation	Cotter, W., Morrissey, P.E., Yang, H., O'Callaghan, J., Roycroft, B., Corbett, B. and Peters, F.H., 2019. Integrated demultiplexing and amplification of coherent optical combs. Optics express, 27(11), (12pp). DOI:10.1364/OE.27.016012
Type of publication	Article (peer-reviewed)
Link to publisher's version	https://www.osapublishing.org/oe/abstract.cfm?uri=oe-27-11-16012 - 10.1364/OE.27.016012
Rights	© 2019 Optical Society of America under the terms of the OSA Open Access Publishing Agreement - https://creativecommons.org/licenses/by/4.0/
Download date	2026-11-17 08:36:35
Item downloaded from	https://hdl.handle.net/10468/9122

UCC
University College Cork, Ireland
Coláiste na hOllscoile Corcaigh

Research Article | Vol. 27, No. 11 | 27 May 2019 | OPTICS EXPRESS 16012
Optics EXPRESS

Integrated demultiplexing and amplification of coherent optical combs

W. COTTER,[1] P. E. MORRISSEY,[2] H. YANG,[3] J. O'CALLAGHAN,[4] B. ROYCROFT,[4] B. CORBETT,[4] AND F. H. PETERS[1,2,*]

[1] *Physics Department, University College Cork, College Road, Cork, Ireland*
[2] *Photonics Packaging Group, Tyndall National Institute, Dyke Parade, Cork, Ireland*
[3] *Integrated Photonics Group, Tyndall National Institute, Dyke Parade, Cork, Ireland*
[4] *Photonic Devices Group, Tyndall National Institute, Dyke Parade, Cork, Ireland*
[*] *f.peters@ucc.ie*

Abstract: The explosive growth of the internet during the last few decades has been enabled by two complementary innovations in optical communications: the use of multiple optical channels within a single optical fibre, and the increase in the bandwidth of individual channels to hundreds of Gbps. Further increases in overall bandwidth look to be provided by more spectrally efficient optical superchannels that use coherent sub-carriers generated using optical orthogonal frequency division multiplexing (OFDM). Yet, a cost effective way of generating these signals has not been demonstrated. One crucial, but missing piece is an effective means to separate the closely frequency spaced optical sub-carriers from the coherent optical comb before placing information on each sub-carrier, and thus creating the OFDM signal. Here, we demonstrate a flexible strategy implemented in a compact photonic integrated circuit (PIC) that is used to separate and amplify these sub-carriers using on-chip injection locking.

© 2019 Optical Society of America under the terms of the OSA Open Access Publishing Agreement

1. Introduction

Coherent optical frequency combs are of great interest to fields as diverse as high speed optical communications [1], metrology [2], [3] and optical clocks [4]. As the worldwide demand for communication bandwidth increases, the importance of using these coherent optical combs to create spectrally efficient coherent optical communications systems is also becoming increasingly important.

Since the internet was formed, the worldwide communication infrastructure has been able to accommodate the necessary growth using multiple discrete optical frequencies in a single optical fibre (wavelength division multiplexing - WDM), and by increasing the data rate through each optical frequency. This method of growth can no longer be maintained as the available frequencies in the optical fibre have now been filled. Additional frequencies can no longer be added, and the current optimised channel rate of 100 Gbps for long haul systems fills the 50 GHz channel allocated in the International Telecommunications Union (ITU) grid, as shown in Fig. 1(a). These 100Gbps signals are typically formed using two polarisations with quadrature phase shift keying (QPSK) at a baud rate of 28 GBd.

The expectation is that the channel rate will continue to increase to 400 Gbps, and beyond into terabits per second (Tbps). The currently accepted 100-400 Gbps solutions provide a practical limit for a single optical carrier or optical channel and thus higher bandwidths have been demonstrated by combining multiple incoherent carriers or wavelengths into superchannels (i.e. Infinera at 500 Gbps [5]) as shown in Fig. 1(b). Since all of the mutually incoherent laser sources are on the same photonic integrated circuit (PIC), it is assumed that any frequency drift of the laser sources will be common in the PIC, and therefore the guard bands can be eliminated. This provides an increase in the information spectral density of the communications. However, in order to maximise the data throughput in an optical fibre for long haul communications, the most

#361322 https://doi.org/10.1364/OE.27.016012
Journal © 2019 Received 9 Apr 2019; accepted 23 Apr 2019; published 21 May 2019

Optics EXPRESS

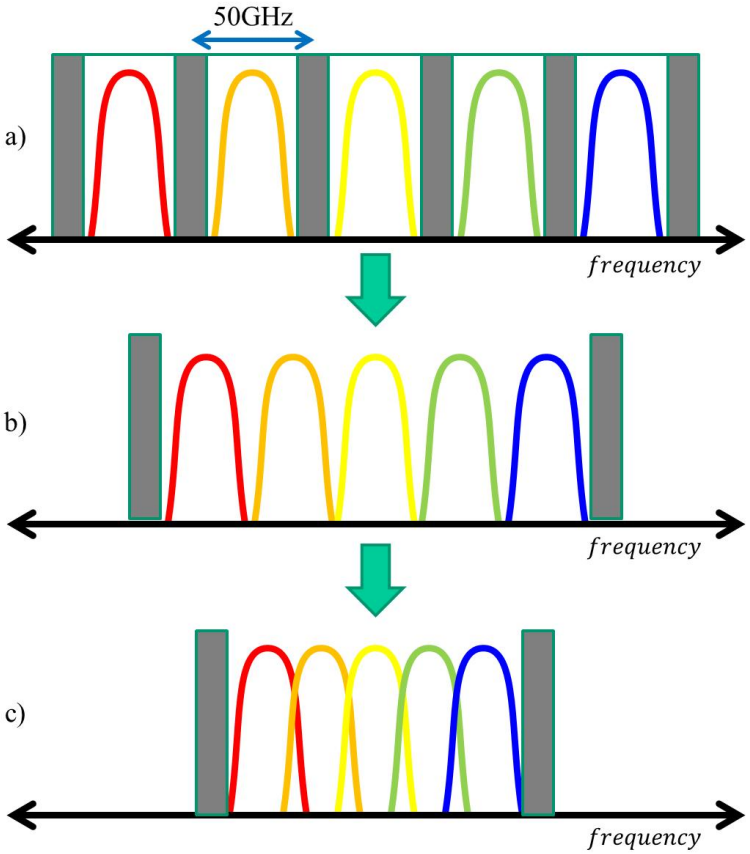


Fig. 1. (a) 100 Gbps per channel using the ITU grid with PM-QPSK and 50 GHz channel spacing. (b) A superchannel based on incoherent sources on a photonic integrated circuit, using 100 Gbps PM-QPSK modulation. (c) A coherent superchannel based on coherent optical comb, using 100 Gbps PM-QPSK modulation and resulting in a higher spectral efficiency

spectrally efficient solutions have used polarisation multiplexed coherent superchannels based on orthogonal frequency division multiplexing (OFDM) [6–9] . The use of coherence between the carriers allows the carriers to overlap, resulting in an increase in the spectral density. This optimised solution can be seen in Fig. 1(c).

For a multi-carrier solution, a coherent optical comb must be generated (Fig. 2(a) and demultiplexed into individual carriers (Fig. 2(b). Data is then placed on the individual carriers (Fig. 2(c) which are then recombined into a single polarisation (Fig. 2(d). Prior to this recombination, and depending on the design, it may be required to adjust the relative phases of each channel. This is repeated for the orthogonal polarisation and the two polarisations are also combined to form the superchannel.

Terabit signals are possible using a high baud rate and multiple bits/symbol with a single optical carrier [10]. However, as the baud rate or the bits/symbol increases, more sophisticated electronic dispersion compensation (EDC) is required for a long haul optical transmission link. Alternatively, terabit signals can be generated using multiple closely spaced coherent optical carriers, where much lower baud rates can be used on each carrier. These multicarrier approaches allow for great flexibility in terms of baud rate and modulation format, thus enabling longer

Optics EXPRESS

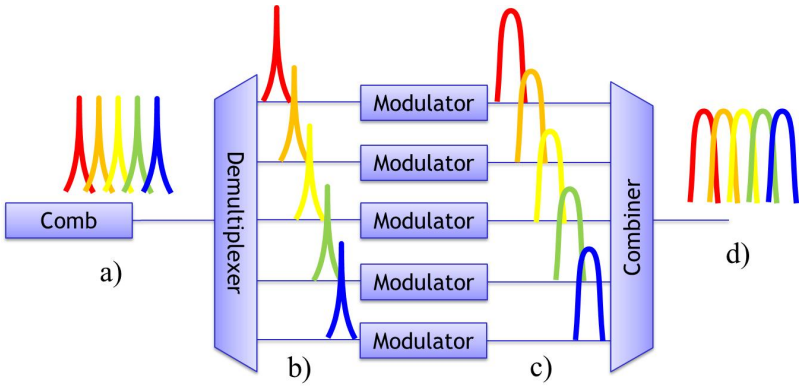


Fig. 2. This schematic describes how on polarisation of an optical OFDM signal can be generated (a) A comb source is used to generate a coherent optical comb at a precise spacing. (b) The carrier of the optical comb are separated into individual channels. (c) Data is put onto each carrier using an optical modulator. (d) The modulated carriers are combined into the OFDM signal. In addition, each carrier may require additional phase control.

distance transmission using lower speed electronics and photonics [11]. If the relative coherence is retained then EDC can be avoided at low baud rates, while some non-linear transmission effects can be greatly reduced [1]. However, prior to this work a means of assembling such a superchannel based on closely spaced <12.5 GHz optical combs has not been feasible, due to the difficulty of demultiplexing the comb while retaining relative coherence between the optical carriers. The technique has the additional advantage of tunability and inherent wavelength tracking, due to the injection locking process.

These optical carriers have been produced by using various techniques including mode-locked lasers [12] or cascaded modulators [13–16]. However, in order to modulate the individual carriers the comb must be demultiplexed. The focus of this paper is therefore to demonstrate a solution for demultiplexing closely spaced optical carriers using a InP PIC, while providing the additional advantage of retaining the mutual coherence between the comb lines within the PIC. The technique has the additional advantage of tunability and inherent wavelength tracking, due to the injection locking process.

1.1. The challenge of demultiplexing closely spaced coherent channels

Figure 2 provides a schematic of how an optical OFDM superchannel can be constructed. All of the required pieces are readily available with the exception of an effective means to demultiplex the signal. There are a number of fibre based technologies that can be used to separate the closely spaced optical channels used in an OFDM signal, but without extensive thermal control, the relative phases between different channels cannot be maintained, rendering those solutions impractical. Optical demultiplexing of wavelengths can also be performed using spectrometers which are implemented in a compact, chip-scale manner where the phase stability is managed due to the single photonic chip. Examples of chip based demultiplexers include: cascaded interferometers [17, 18] Echelle gratings [19, 20], thin-film filters [21] and arrayed waveguide gratings (AWG) [22, 23].

The most common way of demultiplexing a WDM signal consisting of a large number of closely spaced frequencies is to use an AWG, but this is not a viable solution for highly spectrally efficient OFDM signals. In an OFDM signal, the channel separation must be an integer (or half integer) multiple of the clock frequency of the modulation. If an excessive dispersion penalty is to be avoided, clock rates of 25 GHz or less are ideal. However, AWGs scale rapidly with decreasing

free spectral range and thus even a 25 GHz AWG implemented in a high index waveguide material, such as Silicon or InP, is very large, with a footprint of 6mm x 6mm (shown in Fig. 3(b)). This would add considerably to the size and cost of a PIC. Asymmetric Mach-Zehnder interferometers (AMZI) are also used to demultiplex coherent comb sources and very good performance has been reported [18]. However in order to filter a signal with 25 GHz carrier separation, the length difference between the arms in a MZI would be approximately 40 mm using InP technology. Spiral waveguides can be used to reduce the device size and with a minimum radius of curvature of 350 μm the footprint can be reduced to 4.5 mm x 3.5 mm (Fig. 3(c)). In order to bring the size of such a configuration in line with the size of the PIC implementation shown in Fig. 3(d), the minimum bend radius would have to be reduced to 50 μm, which would require a deep etch ridge on InP, which, in turn, would result in a significant insertion loss over 40 mm. Successful implementations of this method have been demonstrate using large planar lightwave circuits, [24, 25], but this solution does not allow a full monolithically integrated implementation of a transmitter PIC. The work presented here seeks rather to investigate compact techniques for demultiplexing closely spaced channels, which can be integrated into a larger transmitter PIC.

Reducing the frequency spacing of the comb to 12.5 GHz or less only exacerbates the problem. An AWG implementation would increase in size by a factor of four or more compared to the 25 GHz solution. For example a very impressive arbitrary waveform PIC was made based on 10 GHz spacings [26]. However this was much larger (30 mm $\times$ 35 mm) than any InP PIC commercially available for low cost optical communications. In contrast, this work seeks to demonstrate a simple, small, and therefore low cost solution for coherent demultiplexing. Reducing the comb spacing for the AMZI solution would require a path length difference of at least 80 mm, thus increasing the insertion loss penalty as well as further increasing the size of the component.

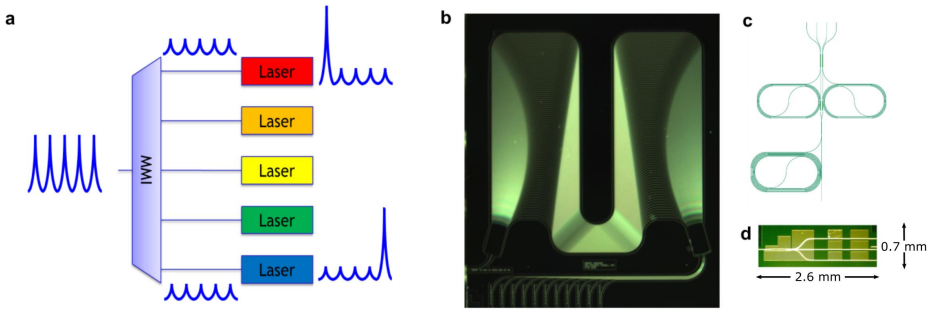


Fig. 3. (a) schematic of the integrated device. The to-scale size comparison of frequency demultiplexing devices: (b) an 25 GHz arrayed waveguide grating fabricated on InP, (c) a 4 channel 25 GHz Mach-Zehnder interferometer (MZI) designed for InP, and (d) the device featured in this paper.

2. A photonic integrated circuit for coherent demultiplexing

In this paper, we describe and demonstrate a completely new type of PIC device used to demultiplex and amplify the coherent combs while maintaining coherence. Active filters are used as the mechanism for demultiplexing the input signal; a technique which has been demonstrated with various laser types previously [27–31]. Injection locking has also been implemented in a PIC that integrated a multimode interference coupler (MMI) with two DFB laser, and was used to generate high purity RF signals. [32] Our device uses this same principle to demultiplex an optical comb, but requiring less devices and integration than required in [32]. It consists of a MMI integrated with an array of tunable lasers shown schematically in Fig. 3(a), and operates in

the following way:

A coherent comb of channels generated off chip is coupled to an input waveguide on the left hand side. This comb propagates through the MMI and is split with equal power coupling to each of the output waveguides, each of which contains a laser. Five output waveguides are shown in Fig. 3(a) for illustration purposes. It is important to note here that no demultiplexing/filtering has taken place at this stage. The lasers are tuned so that only one of the comb lines (carriers) satisfies a resonant condition with each of the lasers. In this way each of the lasers is injection locked with a different comb line and thus the comb is demultiplexed. As the lasers are injection locked, the loss from the MMI is compensated by the injection locked lasers. The coherence between the filtered lines is also maintained due to the monolithic integration of the device and the short waveguides. The footprint of the device featured in this work was 2.6 mm x 0.7 mm (Fig. 3(d). Subsequent designs will use deep etched high curvature Euler bends, further reducing the device size [33]. The device images in Figs. 3b, 3(c), and 3(d) are all shown to the same relative scale.

Slotted Fabry-Pérot (SFP) lasers [34–38] were chosen for the laser array as they can offer single mode performance [34, 38] and tunability by arranging the position and number of slots in the device. They have been shown to function effectively as injection locked active filters [39] and demonstrate stable locking under low injection powers (-20 dBm). Crucially, in order for the lasers to be integrated within a PIC, the slotted Fabry-Pérot lasers can be designed in such a way so that arrays of slots can be used to replace one or both cleaved mirrors. In addition, SFP lasers can be fabricated without requiring any epitaxial re-growth or overgrowth [40]. Both these attributes allow for easy integration with other photonic components, while the single growth stage enables the devices to be readily compatible with commercial foundry processes.

3. Photonic integrated circuit design

Figure 4(a) shows a simplified model of the PIC. Waveguiding sections included a pseudo-passive MMI, S-bend sections and the active (i.e. laser) sections of the device. The MMI and S-bend sections of the device would ideally be passive. However, because the device was monolithically integrated and fabricated in a re-growth free process [40], these sections were absorbing to the light emitted by the lasers (and therefore also to any injected light for injection locking). For this reason, electrical contacts were placed on these pseudo-passive sections so that they could be pumped to transparency, thereby negating material absorption losses.

A single input waveguide on the left accepts the coherent comb signal. The MMI was then used as a power splitter to couple light to each of the lasers in the array through a series of S bends to obtain a separation of 250 μm between laser waveguides so that standard fibre arrays could be used to couple the multiple optical outputs simultaneously. Constant curvature bends were used with a radius of curvature of 350 μm. Large contact pads were implemented for ease of probing.

Based on the optimised 1x3 MMI design, the resulting false colour intensity plot representing the multimode interference pattern as the light travels through the MMI is seen in Fig. 4(b). The MMI width was 22 μm and the length 376 μm. The width of the waveguides in the device were 2.5 μm. This was tapered up to 3.5 μm on the input and output waveguides of the MMI in order to improve coupling effiencies into and out of the multi-mode region of the MMI. The optimised MMI design resulted in a theoretical loss of 16% resulting in a coupling efficiency of 28% of the input power in to each of the output waveguides. The slotted mirror of the lasers are represented in Fig. 4(a). A solitary slot does not provide enough optical feedback to achieve above threshold operation, therefore multiple slots are used. The distance between the slots sets the free spectral range (FSR) of the slotted mirror structure while the number of slots affects the peak reflectivity and the finesse of the mirror. Seven slots were included in the mirror design here with a constant slot-slot distance of 108 μm. The calculated reflection spectrum of the mirror design featured in these lasers is shown in Fig. 4(d). The interslot distance of 108 μm resulted

Optics EXPRESS

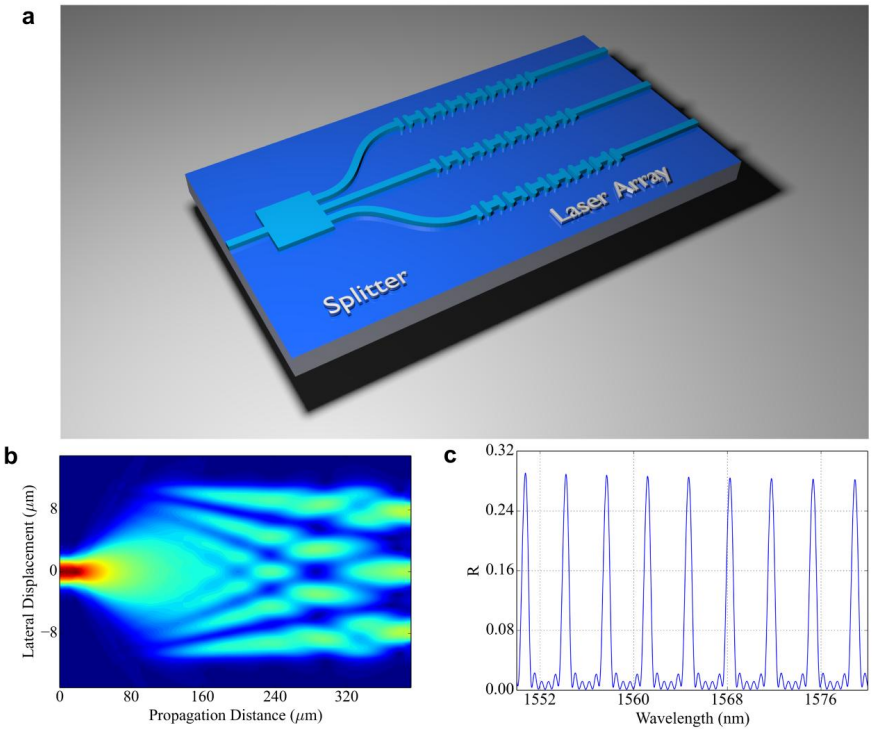


Fig. 4. Images showing the design steps of the device; (a) Schematic of device design, (b) Calculated mode interference in the MMI, (c) Calculated reflection spectrum of the mirror. The reflection peaks are separated by 400 GHz according with the slot separation of 108 μm

in a FSR of approximately 400 GHz as intended for the frequency spacing of superchannels. The peak reflectivity of the mirror was calculated to be 0.28. The second mirror is formed by the cleaved facet. In this particular device the laser gain section length was 700 μm. The gain sections of lasers in a single PIC were exactly the same due to being defined by a single cleave. This ensured similar operation and performance of each of the lasers in the array.

Shallow etched slots angled at 7° were placed in between different sections to provide electrical isolation without added reflections. Typical isolation resistances across a slot amounted to a few $k\Omega$. Separate electrical contacts were defined for both the gain and mirror sections. Adjusting the current in these sections independently facilitated tuning of the precise resonance wavelength of the device.

4. PIC characterisation

The experiment was set up as shown in Fig. 5(a). A tunable laser source (TLS) was used to provide a narrow linewidth (<100 kHz) optical signal. The TLS was tunable from wavelengths of 1520 nm to 1620 nm with a maximum output power of 7 dBm. An isolator was used on the output of the TLS to ensure there were no back reflections into the tunable laser. The TLS output was coupled to a Mach-Zehnder modulator (MZM) in order to produce a coherent comb. This was a packaged commercial MZM with a 3 dB bandwidth of 28 GHz. A polarisation controller was used to ensure correct polarisation for the MZM to operate optimally. The correct polarisation was found using by examining the spectrum of the comb while adjusting the paddles on the polarisation controller. A voltage source was used to set the DC bias across the MZM.

Optics EXPRESS

The DC bias on the MZM was set at the null to produce a comb in a dual sideband suppressed carrier (DS-SC) configuration. A tunable RF signal generator was used to provide the RF signal. In the experiment the output frequency of the generator was set to 12.5 GHz with RF power of 23 dBm, resulting in a two-line comb spaced at 25 GHz. This spacing was chosen for the PIC demonstration, since the different comb lines can be easily seen on an Optical Spectrum Analyser. However, this technique has also been used to successfully demultiplex channels from optical combs with frequency spacings as low as 1 GHz [41].

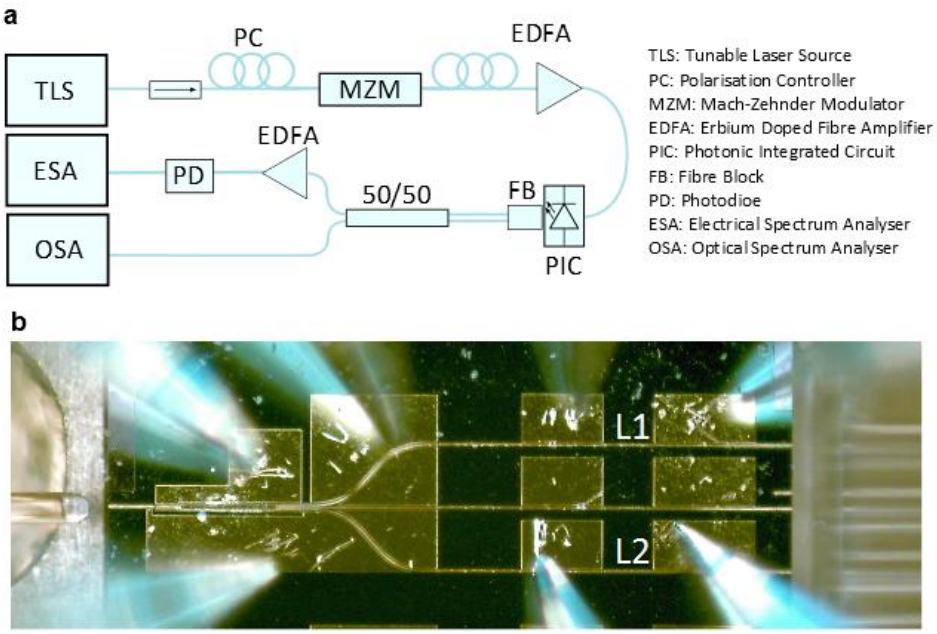


Fig. 5. (a) Schematic of the experimental setup used to test the device which consisted of a tunable laser source (TLS), a Mach-Zehnder modulator (MZM), a Polarisation Controller (PC) an erbium-doped fibre amplifier (EDFA) an multiple fibre block (FB), a high speed photodetector (PD), an electric spectrum analyser (ESA) and an optical spectrum analyser (OSA), (b) The complete device under test. Optical coupling was achieved with a lensed fibre on the input (left) side and a fibre block was used for coupling on the output (right) side. Multiple needle probes were used to contact the various sections of the device.

A second polarisation controller was used to ensure correct polarisation for injection to the PIC. The polarisation was selected by injection locking one of the lasers on the PIC and adjusting the paddles on the controller to maximise suppression of slave laser sidemodes.

An erbium doped fibre amplifier (EDFA) with a maximum output power of 15 dBm and maximum small signal gain of 25 dB was used to boost the signal to account for losses through the MZM. The EDFA was not used at the saturation current. Gain flatness was not a problem in the EDFA as the comb contained only two lines spaced at 25 GHz The integrated circuit was then used to filter, amplify and demultiplex the two-line comb.

A lensed fibre with a working distance of $\tilde{1}0$ μm was used to couple light to the input waveguide of the PIC. To control the location of the lensed fibre tip, an automated alignment system was used. This automated coupling system was beneficial in the experiment as it allowed for high coupling efficiencies but more importantly it allowed for stable, repeatable coupling. Injection locking is sensitive to injected power both in terms of detuning characteristics (or in this case, filter width) and the final SMSR achieved. A 3-axis stage was used with stepper motor actuators

for coarse alignment and piezo actuators for fine control. An optical feedback loop was used to optimise coupling efficiency. Coupling efficiencies of greater than 50% were possible using this alignment system.

A combination of DC voltage and current sources were used to provide current to the various device contacts. Voltage sources were used for the pseudo-passive MMI and S-bend sections, while current sources were used for the lasers. As the input facet of the device was not AR coated a cavity existed between the input facet and the mirror of the lasers with the MMI and S-bends in the middle. This section was tested to see if and at what current it would achieve above threshold laser operation. Lasing threshold was achieved at a current of 180 mA injected to the MMI and S-bends sections. Thus, during the demultiplexing experiment the current in these sections totalled 120 mA; well below the threshold current.

A fibre block was used to couple the multiple outputs simultaneously. The facet of the fibre block was angled to prevent reflections back in to the laser cavity. Positioning of the fibre block was achieved using a 3-axis stage with manual micrometre actuators. A manual positioner could be used here as the absolute coupling power and efficiency did not affect device operation.

Figure 5(b) shows a microscope image of the device under test. The input lensed fibre can be seen on the left side of the image. On the right, a fibre array is used to couple multiple outputs simultaneously. In the centre of the image the probe needles used to provide current to the various device sections are visible.

Figure 6(a) and Fig. 6(b) show the free running spectra of lasers L1 and L2 respectively. L1 had a peak wavelength of 1569.02 nm and an SMSR of 19.6 dB at drive currents of 50 mA in the gain section and 50 mA in the mirror section. These drive currents amounted to $1.3\times I_{th}$. L2 had a peak wavelength of 1569.22 nm with an SMSR of 17.1 dB. L2 drive currents were 65 mA in the gain section and 65 mA in the mirror section which was equal to $1.9\times I_{th}$. The peak carrier wavelengths were separated by 0.2 nm or 25 GHz. Non-lasing wavelengths were then selected for injection locking. The carriers selected for injection were at wavelengths of 1565.76 nm and 1565.96 nm. These modes were also separated by 25 GHz allowing the input comb to be aligned with them. Unlike existing demultiplexing methods that rely on interference, our new design is tunable and is only limited by the tunability of the injection locked laser resonances and the injection locking bandwidth. The design can therefore support optical combs with carriers separated by between 10 and 50 GHz using the same device.

Figure 6(c) shows laser L1 locked to the comb line at 1565.76 nm. The second most prominent peak at a wavelength of 1565.96 nm was the other comb line which was not on resonance with the slave laser. Although not resonant with any of the modes of the laser, the unfiltered comb line still passed through the device without being fully attenuated. We define the comb rejection ratio (CRR) to be the ratio between the power in the demultiplexer comb line and the line with the second most power. For this first line, a CRR of 20.6 dB was achieved. Figure 6(d) shows laser L2 locked to the comb line at 1565.96 nm. An CRR of 19.1 dB was achieved. In this case there were two non lasing peaks of similar power. One was the non-filtered comb line, at a wavelength of 1565.76 nm. The other was at a wavelength of 1569.23 nm which was the lasing mode when not injection locked.

One important thing to note in using this device is the importance of the input power or more precisely the peak powers of each of the comb lines. Looking again at Fig. 6(c) and Fig. 6(d) we can see that a minimum suppression of 19.1 dB was achieved. For these spectra there are two suppression mechanisms to consider. The first is the increase in SMSR of the slave laser due to being injection locked by one of the comb lines. This suppression increases with input power [42]. The second suppression mechanism is the level of filtering of comb lines being achieved using the injection locked laser, where the suppression decreases as the injection power increases. As the injection power is increased the peak power of the "unwanted" lines increases also. Therefore there is an optimum injection power required to maximise SMSR at the output of

Optics EXPRESS

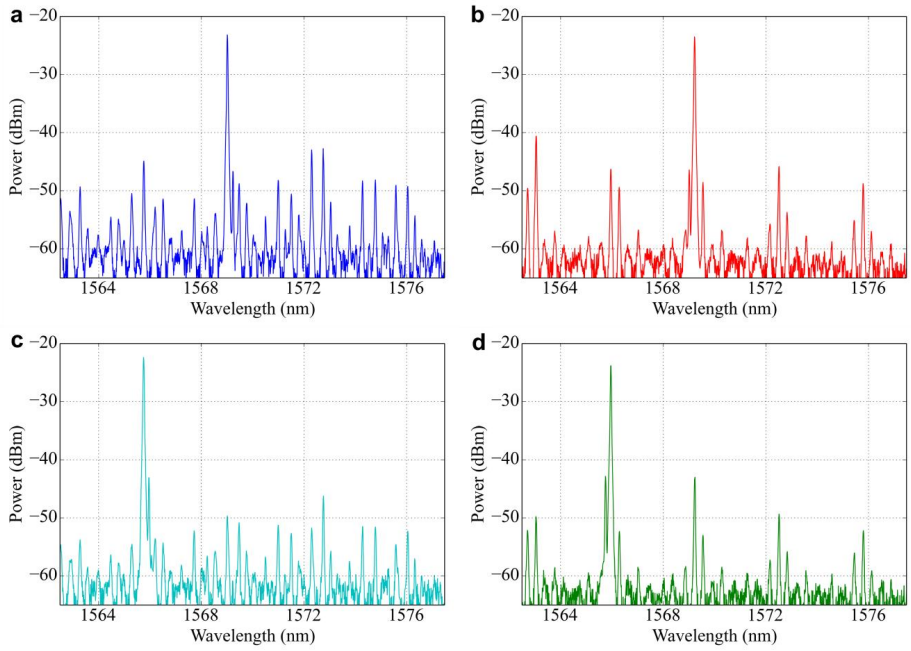


Fig. 6. (a) Laser 1 free running with a peak output of 1569.02 nm. Operating current was at 1.5 Ith (b) Optical spectrum of Laser 2 free running with a peak output of 1569.22 nm. Operating current was 1.9 Ith (c) Output of Laser 1 injection locked by and filtering the comb source line at a wavelength of 1565.76 nm (d) Output of Laser 2 injection locked by an input comb line at a wavelength of 1565.96 nm.

the device. The optimum input power was typically quite low at around -20 dBm peak power for each of the comb lines. While 20 dB comb rejection has been demonstrated, the goal is to reach 30 dB or greater. The current approach to increase the rejection is by using injection locked lasers based on higher Q cavities.

Both Fig. 6(c) and Fig. 6(d) show that it was possible to filter the coherent comb when 25 GHz was maintained between the filtered outputs. In order to test for coherence between filtered lines, the output signals were coupled back together. Figure 7(a) shows the optical spectrum of the recoupled outputs of the device. The power spectrum of the recoupled outputs was also examined on an electrical spectrum analyser (ESA). This was achieved with an EDFA coupled to a non-amplified high speed photodiode. Figure 7(b) shows the beat-note at 25 GHz created by the interaction between the two filtered wavelengths.

The -3dB width of the beat-note was measured to be approximately 5 kHz. This was much narrower than the linewidth of the source laser (100 kHz) and signifies that coherence was maintained between filtered comb lines while on the PIC (although this relative coherence was lost during the experiment due to the optical fibre employed). The narrowing of the linewidth of the beat-note was limited by the 5 kHz resolution bandwidth (RBW) on the ESA.

5. Conclusions

In this paper we have demonstrated a compact PIC used to demultiplex coherent optical combs for enabling compact coherent OFDM Tbps communications. This is the first demonstration of a technique that is tunable and can accommodate comb line separations as low as 10 GHz in a very compact form factor, thus retaining a stable phase relationship between comb lines. In the PIC, a

Optics EXPRESS

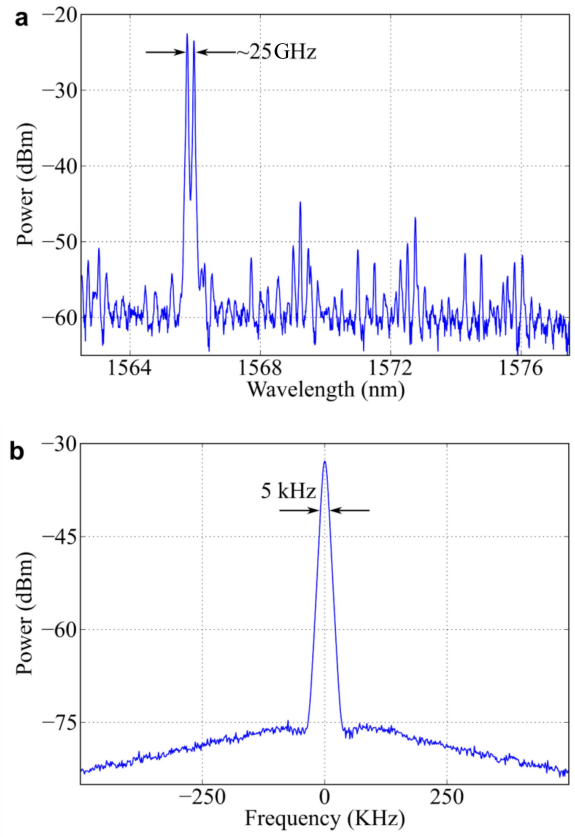


Fig. 7. Optical and power spectra of device with coupled outputs; (a) Optical spectrum of the coupled outputs of Laser 1 and laser two while injection locked, (b) Power spectrum of the beat-note generated from interaction of the two peak wavelength in (a). The linewidth of the beat-note was approximately 5 kHz.

multimode interference coupler was successfully integrated with an array of tunable lasers, and was used to successfully filter a two-line, 25 GHz optical comb. It was demonstrated that the coherence between comb lines was maintained through the filtering process. The scalabilty of the technique is clear by using an MMI with a greater number of output channels (with associated lasers). With a greater number of channels proper passive waveguides for the MMI and S-bends would be beneficial. This could be achieved using more complex fabrication processes using techniques such as quantum well intermixing (QWI) or epitaxial regrowth.

Funding

Science Foundation Ireland under grants SFI 10/CE/I1853 (CTVR2) and SFI 13/IA/1960, and by Enterprise Ireland under grant EI CF 2013 3617B (COMBPIC).

References

1. E. Temprana, E. Myslivets, B. P. -P. Kuo, L. Liu, V. Ataie, N. Alic, and S. Radic, "Overcoming Kerr-induced capacity limit in optical fiber transmission," Science **348**, 1445–1448 (2015).
2. M. J. Thorpe, K. D. Moll, R. J. Jones, B. Safdi, and J. Ye, "Broadband cavity ringdown spectroscopy for sensitive and rapid molecular detection." Science **311**, 1595–1599 (2006).

Optics EXPRESS

3. B. Spaun, P. B. Changala, S. Patterson, B. J. Bjork, O. H. Heckl, J. M. Doyle, and J. Ye, "Continuous probing of cold complex molecules with infrared frequency comb spectroscopy," Nature **533**, 517–520 (2016).
4. Th. Udem, R. Holzwarth, and T. W. Hänsch, "Optical frequency metrology," Nature **416**, 233–237 (2002).
5. F. Kish, "500Gb/s and Beyond PIC-Module Transmitters and Receivers," in *Opt. Fiber Commun. Conf.* W3I.1, OSA, 2014
6. W. Shieh, H. Bao, and Y. Tang, "Coherent optical OFDM: theory and design," Opt. Express **16**, 841–859 (2008).
7. A. J. Lowery, L. B. Du, and J. Armstrong, "Performance of Optical OFDM in Ultralong-Haul WDM Lightwave Systems," J. Lightwave Technol. **25**, 131–138 (2007).
8. J. Armstrong, and A. J. Lowery, "Power efficient optical OFDM," Electron. Lett. **42**, 370–372 (2006).
9. W. Shieh, X. Yi, and Y. Tang, "Transmission experiment of multi-gigabit coherent optical OFDM systems over 1000km SSMF fibre," Electron. Lett. **43**, 183–184 (2007).
10. G. Raybon, A. Adamiecki, J. Cho, P. Winzer, A. Konczykowska, F. Jorge, J-Y. Dupuy, M. Riet, B. Duval, K. Kim, S. Randel, D. Pilori, B. Guan, N. Fontaine, and E. C. Burrows, "Single-carrier all-ETDM 1.08-Terabit/s line rate PDM-64-QAM transmitter using a high-speed 3-bit multiplexing DAC," *IEEE Photonics Conference (IPC)*, Reston, VA, USA, 2015
11. M. D. G. Pascual, R. Zhou, F. Smyth, P. M. Anandarajah, and L. P. Barry, "Software reconfigurable highly flexible gain switched optical frequency comb source," Opt. Express **23**(18), 23225–23235 (2015).
12. H. A. Haus, "Mode-locking of lasers," IEEE J. Sel. Top. Quantum Electron. **6**, 1173–1185 (2000).
13. W. Mao, P. A. Andrekson, and J. Toulouse, "Investigation of a spectrally flat multi-wavelength DWDM source based on optical phase- and intensity-modulation," in *Opt. Fiber Commun. Conf.* MF78, OSA, (2004).
14. T. Morioka, K. Mori, and M. Saruwatari, "More than 100-wavelength-channel picosecond optical pulse generation from single laser source using supercontinuum in optical fibres," Electron. Lett. **29**, 862–864 (1993).
15. T. Sakamoto, T. Kawanishi, and M. Izutsu, "Asymptotic formalism for ultraflat optical frequency comb generation using a Mach-Zehnder modulator," Opt. Lett. **32**, 1515–1517 (2007).
16. L. Zhang, Y. Song, S. Zou, Y. Li, J. Ye, and R. Lin "Flat frequency comb generation based on Mach-Zehnder modulator and phase modulator," in *IEEE 12th Int. Conf. Commun. Technol.*, 2010.
17. B. H. Verbeek, C. H. Henry, N. A. Olsson, K. J. Orlowsky, R. F. Kazarinov, and B. H. Johnson, "Integrated four-channel Mach-Zehnder multi/demultiplexer fabricated with phosphorous doped SiO_2 waveguides on Si," J. Lightwave Technol. **6**, 1011–1015 (1998).
18. K. Nara, H. Urabe, J. Hasegawa, N. Matsubara, and H. Kawashima, "MZI based 8-channel wideband WDM filter array with low loss ripple and high isolation using silica-based PLC [planar lightwave circuits]," in *OFC/NFOEC Tech. Dig. Opt. Fiber Commun. Conf.* (2005).
19. S. Janz, "Planar Waveguide Echelle Gratings in Silica-On-Silicon," IEEE Photonics Technol. Lett. **16**, 503–505 (2004).
20. P. C. Clemens, G. Heise, R. Marz, H. Michel, A. Reichelt, and H. W. Schneider, "8-channel optical demultiplexer realized as SiO_2/Si flat-field spectrograph," IEEE Photonics Technol. Lett. **6**, 1109–1111 (1994).
21. J. Minowa, and Y. Fujii, "Dielectric multilayer thin-film filters for WDM transmission systems," J. Lightwave Technol. **1**, 116–121 (1983).
22. C. Dragone, C. "An N*N optical multiplexer using a planar arrangement of two star couplers," IEEE Photonics Technol. Lett. **3**, 812–815 (1991).
23. S. Chandrasekhar, S. M. Zirngibl, A. G. Dentai, C. H. Joyner, F. Storz, C. A. Burrus, and L. M. Lunardi, "Monolithic eight-wavelength demultiplexed receiver for dense WDM applications," IEEE Photonics Technol. Lett. **7**, 1342–1344 (1995).
24. K. Takiguchi, M. Oguma, T. Shibata, and H. Takahashi, "Demultiplexer for optical orthogonal frequency-division multiplexing using an optical fast-Fourier-transform circuit," Opt. Lett. **34**, 1828âĂŞ-1830 (2009).
25. D. Hillerkuss, M. Winter, M. Teschke, A. Marculescu, J. Li, G. Sigurdsson, K. Worms, S. Ben Ezra, N. Narkiss, W. Freude, J. Leuthold, "Simple all-optical FFT scheme enabling Tbit/s real-time signal processing," Opt. Express **18**, 9329–9340 (2010).
26. Francisco M. Soares, Nicolas K. Fontaine, Ryan P. Scott, J. H. Baek, X. Zhou, T. Su, S. Cheung, Y. Wang, C. Junesand, S. Lourdudoss, K. Y. Liou, R. A. Hamm, W. Wang, B. Patel, L. A. Gruezke, W. T. Tsang, Jonathan P. Heritage, S. J. B. Yoo, "Monolithic InP 100-Channel × 10-GHz Device for Optical Arbitrary Waveform Generation" IEEE Photonics Journal **3**, 975–985 (2010).
27. M. Nishio, T. Numai, S. Suzuki, M. Fujiwara, M. Itoh, and S. Murata, "Eight-channel wavelength-division switching experiment using wide-tuning-range DFB LD filters," in *Eur. Conf. Opt. Commun.* (1988).
28. H. Kawaguchi, K. Magari, K. Oe, Y. Noguchi, Y. Nakano, and G. Motosugi, "Optical frequency-selective amplification in a distributed feedback type semiconductor laser amplifier," Appl. Phys. Lett. **50**, 66–67 (1987).
29. K. Kikuchi, C.-E. Zah, and T.-P. Lee, "Amplitude-modulation sideband injection locking characteristics of semiconductor lasers and their application," IEEE J. Lightwave Technol. **6**, 1821–1830 (1988).
30. C. F. C. Silva, A. J. Seeds, and P. J. Williams, "Terahertz span >60-channel exact frequency dense WDM source using comb generation and SG-DBR injection-locked laser filtering," IEEE Photonics Technol. Lett. **13**, 370–372 (2001).
31. A. Dentai, J. Stone, E. C. Burrows, C. A. Burrus, L. W. Stulz, and M. Zirngibl "Electrically tunable semiconductor Fabry-Perot filter," IEEE Photonics Technol. Lett. **6**, 629–631 (1994).
32. Katarzyna Balakier, Martyn J. Fice, Frederic van Dijk, Gael Kervella, Guillermo Carpintero, Alwyn J. Seeds, and

Optics EXPRESS

Cyril C. Renaud, "Optical injection locking of monolithically integrated photonic source for generation of high purity signals above 100 GHz," Opt. Express **22**, 29404–29412 (2014).
33. R. N. Sheehan, S. Horne, and F. H. Peters, "The design of low-loss curved waveguides," Opt. Quantum Electron. **40**, 1211âĂŞ-1218 (2008).
34. J.-P. Engelstaedter, B. Roycroft, F. H. Peters, and B. Corbett, "Design of Tuneable Laser With Interleaved Sampled Grating Rear Mirror," J. Lightwave Technol. **28**, 2830–2835 (2010).
35. Q. Lu, W.-H. Guo, D. Byrne, and J. F. Donegan, "Design of Slotted Single-Mode Lasers Suitable for Photonic Integration," IEEE Photonics Technol. Lett. **22**, 787–789 (2010).
36. L. Coldren, K. Ebeling, B. Miller, and J. Rentschler, "Single longitudinal mode operation of two-section GaInAsP/InP lasers under pulsed excitation," IEEE J. Quantum Electron. **19**, 1057–1062 (1983).
37. B. Corbett, and D. McDonald, "Single longitudinal mode ridge waveguide 1.3 µm Fabry-Perot laser by modal perturbation," Electron. Lett. **31**, 2181–2182 (1995).
38. S. K. Mondal, B. Roycroft, P. Lambkin, F. Peters, B. Corbett, P. Townsend, and A. Ellis "A Multiwavelength Low-Power Wavelength-Locked Slotted Fabry-Perot Laser Source for WDM Applications," IEEE Photonics Technol. Lett. **19**, 744–746 (2007).
39. W. Cotter, D. Goulding, B. Roycroft, J. O'Callaghan, B. Corbett, and F. H. Peters "Investigation of active filter using injection-locked slotted Fabry-Perot semiconductor laser," Appl. Opt. **51**, 7357–7361 (2012).
40. H. Yang, P. Morrissey, W. Cotter, C. L. M. Daunt, J. O'Callaghan, B. Roycroft, N. Ye, N. Kelly, B. Corbett, F. H. Peters, (2013) "Monolithic Integration of Single Facet Slotted Laser, SOA, and MMI Coupler," IEEE Photonics Technol. Lett. **25**, 257–260 (2013).
41. K. Shortiss, A. H. Perrot, M. Shayesteh, M. Dernaika, F. Dubois and F. H. Peters, "Integrated optical demultiplexing by injection locking," *Photonics Ireland*, Cork, Ireland, 2018
42. M. M. Krstić, and D. M. Gvozdić, "Side-Mode-Suppression-Ratio of Injection-Locked Fabry âĂŞ Perot Lasers," in *Proceedings of the International School and Conference on Photonics, PHOTONICA09* 116, pp. 664–667 (2009).

143.239.102.117 {ts '2019-06-26 10:59:36'}